

# Compton Scattering from the Deuteron and Extracted Neutron Polarizabilities

M. Lundin,<sup>1</sup> J.-O. Adler,<sup>1</sup> M. Boland,<sup>1</sup> K. Fissum,<sup>1</sup> T. Glebe,<sup>2</sup> K. Hansen,<sup>1</sup> L. Isaksson,<sup>1</sup> O. Kaltschmidt,<sup>2</sup> M. Karlsson,<sup>1</sup> K. Kossert,<sup>2</sup> M.I. Levchuk,<sup>3</sup> P. Lilja,<sup>1</sup> B. Lindner,<sup>4</sup> A.I. L'vov,<sup>5</sup> B. Nilsson,<sup>1</sup> D.E. Oner,<sup>2</sup> C. Poech,<sup>2</sup> S. Proff,<sup>2</sup> A. Sandell,<sup>1</sup> B. Schröder,<sup>1</sup> M. Schumacher,<sup>2</sup> and D.A. Sims<sup>1</sup>

<sup>1</sup>*Department of Physics, University of Lund, SE-22100 Lund, Sweden*

<sup>2</sup>*Zweites Physikalisches Institut, Universität Göttingen D-37073 Göttingen, Germany*

<sup>3</sup>*B.I. Stepanov Institute of Physics, Belarussian Academy of Sciences, 220072 Minsk, Belarus*

<sup>4</sup>*Kristianstad University College, SE-29188 Kristianstad, Sweden*

<sup>5</sup>*P.N. Lebedev Physical Institute, 119991 Moscow, Russia*

(Dated: November 3, 2018)

Differential cross sections for Compton scattering from the deuteron were measured at MAX-lab for incident photon energies of 55 MeV and 66 MeV at nominal laboratory angles of 45°, 125°, and 135°. Tagged photons were scattered from liquid deuterium and detected in three NaI spectrometers. By comparing the data with theoretical calculations in the framework of a one-boson-exchange potential model, the sum and difference of the isospin-averaged nucleon polarizabilities,  $\alpha_N + \beta_N = 17.4 \pm 3.7$  and  $\alpha_N - \beta_N = 6.4 \pm 2.4$  (in units of  $10^{-4} \text{ fm}^3$ ), have been determined. By combining the latter with the global-averaged value for  $\alpha_p - \beta_p$  and using the predictions of the Baldin sum rule for the sum of the nucleon polarizabilities, we have obtained values for the neutron electric and magnetic polarizabilities of  $\alpha_n = 8.8 \pm 2.4(\text{total}) \pm 3.0(\text{model})$  and  $\beta_n = 6.5 \mp 2.4(\text{total}) \mp 3.0(\text{model})$ , respectively.

PACS numbers: 25.20.Dc, 13.40.Em, 13.60.Fz, 14.20.Dh

The electric ( $\alpha$ ) and magnetic ( $\beta$ ) polarizabilities of the nucleon characterize the second-order response of its internal structure to applied electric and magnetic fields, respectively. Since the polarizabilities manifest themselves in two-photon processes, an excellent method to measure them is via Compton scattering experiments.

The most recent global average [1] for the difference of the proton polarizabilities is

$$\alpha_p - \beta_p = 10.5 \pm 0.9(\text{stat} + \text{syst}) \pm 0.7(\text{model}), \quad (1)$$

in units of  $10^{-4} \text{ fm}^3$  (which will be used throughout this paper). The sum of the nucleon polarizabilities is usually obtained indirectly via the predictions of the Baldin sum rule. A recent re-evaluation of this sum rule [2] gives

$$\alpha_p + \beta_p = 14.0 \pm 0.3, \quad (2)$$

$$\alpha_n + \beta_n = 15.2 \pm 0.5. \quad (3)$$

Electromagnetic scattering of low-energy neutrons in the electric fields of heavy nuclei was used to extract  $\alpha_n$  (see Ref. [4] and the references therein). There have been many attempts to measure  $\alpha_n$  using this method [3, 5, 6, 7], but the final conclusion regarding its value has remained unclear. Note that this method does not constrain  $\beta_n$ .

Scattering real photons from neutrons bound in nuclei is another way to measure the neutron polarizabilities. The use of a deuterium target permits the theoretical uncertainties in the interpretation of the experimental data to be minimized. Both the reactions  $\gamma d \rightarrow \gamma np$  (quasi-free) and  $\gamma d \rightarrow \gamma d$  (elastic) can be considered. The suggestion to exploit the quasi-free kinematic region

was made in Refs. [8, 9]. An advantage of this approach is that it can be carefully tested by comparing measured quasi-free proton cross sections with available free-proton data. The method has been used in a series of experiments at MAMI [10, 11, 12] and SAL [13]. The values for the neutron polarizabilities found in these experiments are in agreement with each other; however, the sizes of the quoted errors differ markedly. The most accurate values to date have recently been reported in Ref. [12] as

$$\alpha_n = 12.5 \pm 1.8(\text{stat})_{-0.6}^{+1.1}(\text{syst}) \pm 1.1(\text{model}), \quad (4)$$

$$\beta_n = 2.7 \mp 1.8(\text{stat})_{-1.1}^{+0.6}(\text{syst}) \mp 1.1(\text{model}). \quad (5)$$

The anti-correlated errors in Eqs. (4) and (5) are due to the application of the sum-rule result (3). In view of the model errors contained in Eqs. (4) and (5), confirmation of these values is of great importance.

Elastic photon scattering from the deuteron provides a third experimental method for determining the neutron polarizabilities. While only the isospin-averaged nucleon polarizabilities  $\alpha_N = (\alpha_p + \alpha_n)/2$  and  $\beta_N = (\beta_p + \beta_n)/2$  can be measured, this is not a major problem since the proton values are rather accurate (see Eqs. (1) and (2)). Although the first such measurements of elastic  $\gamma d$  scattering were performed many years ago (see Ref. [14] and the references therein), only two recent experiments at Illinois at  $E_\gamma = 49$  and 69 MeV [15] and at SAL at  $E_\gamma = 94$  MeV [16] have been precise enough to reveal the effect of the nucleon polarizabilities. However, the values for  $\alpha_N - \beta_N$  extracted from these measurements are inconsistent. With the use of the theoretical model [2], a value of  $2.6 \pm 1.8$  was obtained in Ref. [16] that together with Eq. (1) gives  $\alpha_n - \beta_n \simeq -5.3 \pm 3.8$ . But to describe

the data from Ref. [15], one needs to increment  $\alpha_N - \beta_N$  to  $7.9 \pm 3.8$ , thus giving  $\alpha_n - \beta_n = 5.3 \pm 7.6$ . The former value is far from theoretical estimates of this quantity based on dispersion relations, which crudely predict that  $\alpha_n - \beta_n \simeq \alpha_p - \beta_p$  (see Refs. [17, 18, 19]). It also contradicts the results obtained from quasi-free neutron Compton scattering (see Eqs. (4) and (5)).

In this Letter, we report a new measurement of the differential cross section for deuteron Compton scattering performed at MAX-lab. The near-continuous, 95 MeV electron beam from the MAX I stretcher ring was used to produce tagged photons, in the energy range 50-72 MeV, with an FWHM energy resolution of  $\sim 330$  keV and a flux of about  $3 \times 10^5$  MeV $^{-1}$ s $^{-1}$  [20, 21]. The post-bremsstrahlung electrons were momentum analysed in a magnetic spectrometer using two 32 scintillator hodoscopes located along the focal plane. They were placed such that the central tagged-photon energies were 55 MeV and 66 MeV. The photon beam was incident upon a scattering chamber containing liquid deuterium in a cylindrical cell (length 160 mm and diameter 48 mm) [22] made from 125  $\mu$ m thick Kapton foil.

Scattered photons were detected in three spectrometers, each containing a central NaI detector 25.4 cm in diameter and with depths of either 25.4 or 35.5 cm, placed at nominal lab angles of 45°, 125°, and 135° at a distance of approximately 0.4 m from the target. The resulting solid angle (together with the detection efficiency) was precisely determined via GEANT simulations. The energy resolution of the NaI spectrometers ranged from 6 to 8% at a photon energy of 60 MeV. The gain stability of the NaI detectors was continuously monitored and instabilities were corrected for using a Light Emitting Diode (LED) system [23]. In turn, the stability of the LED system was monitored and verified by examining the location of the cosmic peak on a run-by-run basis. The data acquisition was started by an event in any one of the NaI detectors, which provided gates for charge integrating ADCs (Analog to Digital Converter) and start signals for TDCs (Time to Digital Converter) used for time-of-flight (TOF) measurements. The stop signals for the TDCs came from the focal-plane detectors. In order to monitor the number of pile-up events in the NaI crystals, a 250 MHz Flash ADC was used. Less than 1% of the events were affected by pile-up.

Data were collected over 8 weeks, divided typically into two-week run periods. For each run period, tagging efficiencies ( $\sim 20\%$ ) were measured using a Pb/SCIFI detector [24]. In addition, the responses of the NaI spectrometers were measured by placing them directly in the reduced intensity photon beam. For each detector, the aforementioned GEANT simulations were phenomenologically broadened to match the measured responses. This broadening was then folded into second-stage simulations of the in situ responses and solid angles [23]. A typical result is shown by the dashed line in Fig. 1.

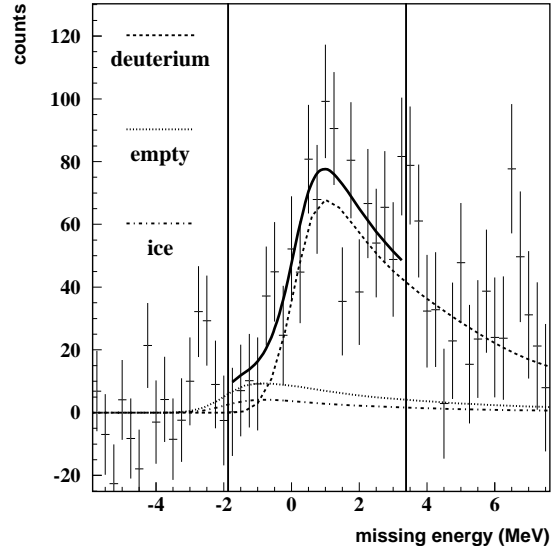


FIG. 1:  $E_{\text{miss}}$  spectrum at  $\theta_{\gamma}^{\text{lab}} = 126^\circ$  and  $E_{\gamma} = 55$  MeV. The two vertical lines indicate the region of interest (ROI) used to determine the yield. The solid line represents the sum of the fitted responses (see text).

This missing energy ( $E_{\text{miss}}$ ) spectrum was obtained by summing over a 10 MeV interval centered at 55 MeV.  $E_{\text{miss}}$  was defined as the difference between the tagged-photon energy (corrected for the Compton scattering energy shift) and the energy registered in the NaI detector. The subtraction of random events was performed using two independent methods: one used the TOF between the scattered photons and the post-bremsstrahlung electrons, while the other employed the non-physical ( $E_{\text{miss}} < 0$ ) region of the energy spectrum. An average normalization factor was employed which resulted in a 4% systematic uncertainty in the extracted cross sections. The experimental data were fitted within the region of interest (ROI) considering the contributions of elastically scattered photons from liquid deuterium, from the Kapton cell and the scattering chamber windows, and from ice ( $\text{H}_2\text{O}$ ) which built up on the cell during the run period. The contribution from the cell and windows was calculated using known differential cross sections for carbon and oxygen [25, 26, 27]. The contribution from ice was fitted using data from the largest detector at the backward angles and extrapolated to the other detector angles. The careful quantification of the experimental background due to the empty target and ice resulted in an average improvement in the  $\chi^2$  of the fit functions of 20% for the backward detector angles. The observed contributions correspond to ice-layer thicknesses of about 100  $\mu$ m per cell endcap. The contribution from inelastic scattering (which begins at  $E_{\text{miss}} = 2.2$  MeV) was kept to less than 3% via the narrow ROI. The systematic uncer-

TABLE I: CM differential cross sections for deuteron Compton scattering. The first uncertainty is statistical and the second is systematic.

| $E_\gamma^{\text{lab}}$ (MeV) | $\Theta_\gamma^{\text{lab}}$ (deg) | $\Theta_\gamma^{\text{CM}}$ (deg) | $d\sigma^{\text{CM}}/d\Omega_\gamma$ (nb/sr) |
|-------------------------------|------------------------------------|-----------------------------------|--|
| 54.6                          | 43.8                               | 44.9                              | $16.8 \pm 4.1 \pm 1.5$                       |
| 54.6                          | 123.7                              | 125.0                             | $15.7 \pm 1.5 \pm 1.3$                       |
| 54.6                          | 135.7                              | 136.8                             | $17.2 \pm 2.0 \pm 1.4$                       |
| 54.9                          | 43.2                               | 44.3                              | $16.6 \pm 3.3 \pm 1.8$                       |
| 54.9                          | 126.3                              | 127.6                             | $15.4 \pm 1.3 \pm 1.0$                       |
| 54.9                          | 135.2                              | 136.3                             | $18.4 \pm 1.7 \pm 1.6$                       |
| 55.9                          | 48.9                               | 50.2                              | $13.4 \pm 2.7 \pm 1.0$                       |
| 55.9                          | 130.4                              | 131.7                             | $15.3 \pm 2.0 \pm 1.2$                       |
| 55.9                          | 136.2                              | 137.3                             | $21.0 \pm 3.2 \pm 2.2$                       |
| 65.3                          | 43.6                               | 44.9                              | $16.0 \pm 2.8 \pm 1.4$                       |
| 65.3                          | 123.7                              | 125.3                             | $15.3 \pm 1.3 \pm 1.4$                       |
| 65.3                          | 135.5                              | 136.8                             | $12.6 \pm 1.7 \pm 1.8$                       |
| 65.6                          | 43.1                               | 44.4                              | $18.6 \pm 2.4 \pm 1.4$                       |
| 65.6                          | 126.3                              | 127.8                             | $16.0 \pm 1.2 \pm 1.1$                       |
| 65.6                          | 135.2                              | 136.5                             | $15.1 \pm 1.7 \pm 1.3$                       |
| 67.0                          | 48.8                               | 50.3                              | $15.2 \pm 1.8 \pm 1.2$                       |
| 67.0                          | 130.3                              | 131.8                             | $14.2 \pm 1.5 \pm 1.0$                       |
| 67.0                          | 136.1                              | 137.5                             | $15.0 \pm 2.7 \pm 1.2$                       |

tainties for the experiment ( $\sim 8\%$ ) arise from the tagging efficiency (5%), the product of the solid angle and the detection efficiency (4%), the random background subtraction (4%), the contamination of the ROI by inelastic photon scattering (3%), and the target thickness (2%).

Results for the center-of-mass (CM) cross sections are given in Table I and displayed in Fig. 2. Earlier results from Illinois [15] and SAL [16] are also shown. Since the Illinois data were obtained at slightly different photon energies (49 MeV and 69 MeV), we extrapolated them to our energies using the theoretical model presented in Ref. [2]. Good agreement with the Illinois data is clearly demonstrated.

The polarizabilities of the nucleon have been determined using the theoretical model presented in Ref. [2]. In this model, apart from effects due to the one-body  $\gamma N$  interaction (which contain the effects due to the polarizabilities), two-body effects due to the  $NN$  interaction and related Meson-Exchange Currents (MEC) have been included via a series of one-boson exchanges which constitute the Bonn potential. After making a two-parameter fit to the data in Table I with the use of this model, we obtain for the sum and difference of the isospin-averaged nucleon polarizabilities

$$\alpha_N + \beta_N = 17.4 \pm 3.7(\text{stat} + \text{syst}), \quad (6)$$

$$\alpha_N - \beta_N = 6.4 \pm 2.4(\text{stat} + \text{syst}), \quad (7)$$

with  $\chi^2/N_{\text{dof}} = 7.5/(18 - 2)$ . The quoted uncertainties are the statistical and systematic uncertainties taken in quadrature. The obtained sum  $\alpha_N + \beta_N$  is in agreement with the values given in Eqs. (2) and (3). This indicates that the systematic uncertainties (including the model uncertainty) are well understood.

Having extracted  $\alpha_N$  and  $\beta_N$ , we invoked the accurate proton values for  $\alpha_p$  and  $\beta_p$  to derive the neutron polarizabilities. In doing this, we relied on the precise sum-rule

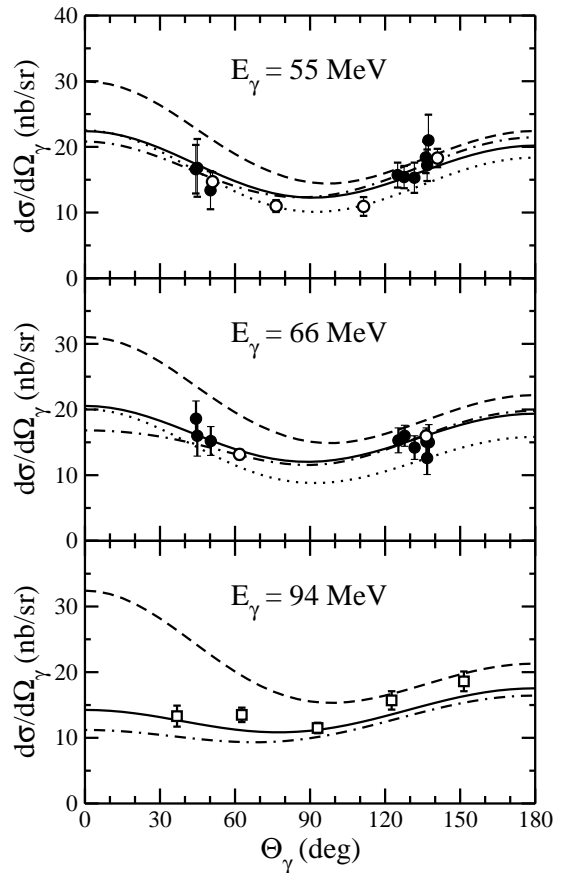


FIG. 2: CM differential cross sections for Compton scattering from the deuteron. Filled circles: present experiment; open circles: extrapolated Illinois results [15] (see text); open squares: SAL results [16]. The error bars represent the quadratic sum of the statistical and systematic uncertainties. Solid and dashed curves are the calculations of Ref. [2] (dashed:  $\alpha_N = \beta_N = 0$ ; solid  $\alpha_N = 11.9$ ,  $\beta_N = 5.5$ , see Eqs. (6), (7)). Dotted and dashed-dotted curves are the predictions of Refs. [28] and [29], respectively, extrapolated to  $\alpha_N = 11.9$ ,  $\beta_N = 5.5$ .

prediction (3) rather than on our result (6). Making use of Eqs. (1)–(3) and (7), we obtain

$$\alpha_n = 8.8 \pm 2.4(\text{stat} + \text{syst}), \quad (8)$$

$$\beta_n = 6.5 \mp 2.4(\text{stat} + \text{syst}). \quad (9)$$

If all currently available data (Illinois, SAL, and Lund) are fit using the theoretical model of Ref. [2], the following “global values” may be inferred:

$$\alpha_N + \beta_N = 16.7 \pm 1.6(\text{tot}), \quad (10)$$

$$\alpha_N - \beta_N = 4.8 \pm 2.0(\text{tot}), \quad (11)$$

with  $\chi^2/N_{\text{dof}} = 38/(29 - 2)$ . Thus, using the Baldin sum rule and Eq. (1),

$$\alpha_n = 7.2 \pm 2.1(\text{tot}), \quad (12)$$

$$\beta_n = 8.1 \mp 2.1(\text{tot}). \quad (13)$$

Here both statistical and systematic uncertainties have been combined, the latter being taken into account through a rescaling of measured cross sections within their normalization uncertainties.

Model uncertainties in the extracted values of the polarizabilities can be partly understood by comparing different calculations of  $d\sigma/d\Omega$  [2, 28, 29, 30, 31, 32]. Fig. 2 shows the three most recent predictions [2, 28, 29] at fixed  $\alpha_N = 11.9$  and  $\beta_N = 5.5$  as given by (6) and (7). At the energies and angles of the present experiment, there is reasonable agreement between the potential model of Ref. [2] and the  $\mathcal{O}(p^4)$  Chiral Perturbation Theory (ChPT) results of Ref. [29]. At the SAL energy and angles, this agreement is poorer. Agreement with the  $\mathcal{O}(p^3)$  ChPT calculation of Ref. [28] is worse.

Within the framework of the potential model used here, the main uncertainties which contribute to the extraction of the polarizabilities arise from evaluations of the MEC and seagull terms. The majority of these uncertainties may be collected into the Thomas-Reiche-Kuhn sum rule enhancement parameter  $\kappa$  which determines the magnitude of the seagull contribution [2]. Depending on the  $NN$  potential used (Paris, Bonn, OBEPR, Argonne v18, Nijm93, or CD-Bonn) the value of  $\kappa$  varies from 0.44 to 0.51. This leads to variations in the differential cross section of about 4% which result in variations in the extracted value of  $\alpha_N$  of about  $\pm 1.5$ . We adopt this as an estimate of the model uncertainty in  $\alpha_N$ . Accordingly, the model uncertainty in the derived value of  $\alpha_n$  is about  $\pm 3$ . The model uncertainty in  $\beta_n$  is anticipated to be smaller than that in  $\alpha_n$ , as the changes in  $\kappa$  given above affect  $\beta_N$  to a smaller degree.

The values obtained for  $\alpha_n$  and  $\beta_n$  are in reasonable agreement with those found in quasi-free Compton scattering from the neutron (see Eqs. (4) and (5)). However, we observed the tendency of the technique of elastic Compton scattering from the deuteron to give smaller values for  $\alpha_n - \beta_n$  than did the technique of quasi-free scattering. Predictions for  $\alpha_n$  in the framework of ChPT at  $\mathcal{O}(p^4)$  [33], the heavy baryon ChPT model with the  $\Delta$ -isobar included [34], and the so-called ‘‘covariant dressed K-matrix model’’ [35] give values of  $13.0 \pm 1.5$ , 16.4, and 12.7, respectively. All are somewhat larger than our value. The situation concerning  $\beta_n$  is less clear. Reasonable agreement with ChPT results of  $7.8 \pm 3.6$  [33] and 9.1 [34] is demonstrated. Ref. [35] suggests a noticeably smaller value of 1.8.

In summary, differential cross sections for deuteron Compton scattering have been measured at MAX-lab. The data were used to extract neutron polarizabilities in a model-dependent analysis. The extracted values for  $\alpha_n$  and  $\beta_n$  are consistent with those obtained from the Illinois data [15]; however, they are inconsistent with those resulting from an analysis of the higher energy SAL data [16]. The present analysis thus confirms the previous observations [2, 32] that the available models cannot rec-

oncile data obtained at photon energies of about 60 MeV with those obtained at about 100 MeV.

This project was supported by the Swedish Research Council, the Knut and Alice Wallenberg Foundation, the Crafoord Foundation, the Swedish Institute, the Wenner-Gren Foundation, and the Royal Swedish Academy of Sciences. The participation of the Göttingen group in the experiment was supported by Deutsche Forschungsgemeinschaft.

- 
- [1] V. Olmos de León *et al.*, Eur. Phys. J. A **10**, 207 (2001).
  - [2] M.I. Levchuk and A.I. L’vov, Nucl. Phys. **A674**, 449 (2000); M.I. Levchuk and A.I. L’vov, Nucl. Phys. **A684**, 490 (2001).
  - [3] Yu.A. Aleksandrov, Phys. Part. Nucl. **32**, 708 (2001).
  - [4] Yu.A. Aleksandrov *et al.*, JETP Lett. **4**, 134 (1966).
  - [5] J. Schmiedmayer *et al.*, Phys. Rev. Lett. **66**, 1015 (1991).
  - [6] L. Koester *et al.*, Phys. Rev. C **51**, 3363 (1995).
  - [7] T.L. Enik *et al.*, Sov. J. Nucl. Phys. **60**, 567 (1997).
  - [8] M.I. Levchuk, A.I. L’vov, and V.A. Petrun’kin, FIAN report No. 86, 1986; Few-Body Syst. **16**, 101 (1994).
  - [9] F. Wissmann, M.I. Levchuk, and M. Schumacher, Eur. Phys. J. A **1**, 193 (1998).
  - [10] K.W. Rose *et al.*, Phys. Lett. B **234**, 460 (1990); Nucl. Phys. **A514**, 621 (1990).
  - [11] F. Wissmann *et al.*, Nucl. Phys. **A660**, 232 (1999).
  - [12] K. Kossert *et al.*, Phys. Rev. Lett. **88**, 162301 (2002).
  - [13] N.R. Kolb *et al.*, Phys. Rev. Lett. **85**, 1388 (2000).
  - [14] A. Tenore and A. Verganelakis, Nuovo Cimento **35**, 261 (1965).
  - [15] M.A. Lucas, Ph.D. thesis, University of Illinois, 1994.
  - [16] D.L. Hornidge *et al.*, Phys. Rev. Lett. **84**, 2334 (2000).
  - [17] V.A. Petrun’kin, Sov. J. Part. Nucl. **12**, 278 (1981).
  - [18] A.I. L’vov, Int. J. Mod. Phys. A **8**, 5267 (1993).
  - [19] B.R. Holstein and A.M. Nathan, Phys. Rev. D **49**, 6101 (1994).
  - [20] L.J. Lindgren *et al.*, Nucl. Instrum. Methods Phys. Res. Sect. A **294**, 10 (1990).
  - [21] J.-O. Adler *et al.*, Nucl. Instrum. Methods Phys. Res. Sect. A **388**, 17 (1997).
  - [22] T. Glebe, MSc thesis, Göttingen University, 1993.
  - [23] M. Lundin, Ph.D. thesis, Lund University, 2002.
  - [24] D.W. Hertzog *et al.*, Nucl. Instrum. Methods Phys. Res. Sect. A **294**, 446 (1990).
  - [25] M. Ludwig *et al.*, Phys. Lett. B **274**, 275 (1992).
  - [26] D. Häger *et al.*, Nucl. Phys. **A595**, 287 (1995).
  - [27] S. Proff *et al.*, Nucl. Phys. **A646**, 67 (1999).
  - [28] H.W. Griesshammer and G. Rupak, Phys. Lett. B **529**, 57 (2002).
  - [29] S.R. Beane *et al.*, arXiv:nucl-th/0209002.
  - [30] J.-W. Chen *et al.*, Nucl. Phys. **A644**, 245 (1998).
  - [31] J.J. Karakowski and G.A. Miller, Phys. Rev. C **60**, 014001 (1999).
  - [32] S.R. Beane *et al.*, Nucl. Phys. **A656**, 367 (1999); M. Malheiro *et al.*, arXiv:nucl-th/0111047.
  - [33] V. Bernard, N. Kaiser, and U.-G. Meißner, Phys. Lett. B **319**, 269 (1993).
  - [34] T.R. Hemmert *et al.*, Phys. Rev. D **57**, 5746 (1998).
  - [35] S. Kondratyuk and O. Scholten, Phys. Rev. C **64**, 024005 (2001).